ARTICLE NO. 79-0285R

J 80-006

Calculation of Laminar Separation Bubbles and Their Effect on Airfoil Performance

00001
20004

W. B. Roberts*
Nielsen Engineering & Research, Inc., Mountain View, Calif.

The "bursting" of leading edge laminar separation bubbles that can occur on moderately thick airfoil sections is the cause of sudden large increases in drag, decrease of lift, and change in pitching moment associated with abrupt stall at high angles of attack. This paper describes a semiempirical theory for the description and calculation of the development and bursting of laminar separation bubbles. The semiempirical theory uses an experimental correlation to relate the length of the laminar free shear layer to the freestream turbulence and a modified version of Hortons method to calculate the properties and reattachment position of the turbulent shear layer. The method is used to predict the development of laminar separation bubbles for NACA airfoils. Comparison of these results with NACA experiments shows good agreement.

Nomenclature

C = chord length
C_d = dissipation coefficient, $\frac{2}{\rho U_e^3}\int_0^\infty \tau\left(\frac{\partial u}{\partial z}\right)dz$
$C_{d(m)}$ = mean dissipation coefficient
C_f = friction coefficient, $\tau_w/\frac{1}{2}\rho U_e^2$
CC = correlation coefficient, $\overline{u_1'\cdot u_2'}/\sqrt{\overline{u'^2_1}}\sqrt{\overline{u'^2_2}}$
H = boundary layer shape parameter based on δ^*, δ^*/θ^*
H_e = boundary layer shape parameter based on ϵ, ϵ/θ^*
i = incidence
L = total length of a laminar separated bubble
L_s = macroscale of the inlet turbulence, $\int_0^{x_p} CC\,d(X_p)$
ℓ_1 = distance between separation and transition in a laminar separation bubble
ℓ_2 = distance between transition and reattachment in a laminar separation bubble
P_0 = total or stagnation pressure
q = dynamic head, $\frac{1}{2}\rho U^2$
R_c = Reynolds number based on chord
$R_{\theta(s)^*}$ = momentum thickness Reynolds number at separation
$R_{\ell l}$ = Reynolds number based on ℓ_1
S = distance along a surface
s = the same as S
$T_{u'}$ = inlet turbulence intensity, $\sqrt{\overline{u'^2}}/U_1$
TF = Taylor's turbulence factor, $T_{u'}(C/L_s)^{1/5}$
U = freestream velocity in the direction of the main flow, $U \equiv \bar{U} + u'$
$\bar{U}$ = time averaged component
U_e = local freestream velocity
u = velocity in the boundary layer or free shear layer parallel to U_e
u' = randomly fluctuating component of velocity
x = distance along an x axis or chord line
x_p = probe separation
y = distance normal to x
z = distance normal to s
α = angle of attack
δ^* = displacement thickness
ϵ = energy thickness
θ^* = momentum thickness
ν = kinematic viscosity
Λ_R = reattachment criterion
ρ = density

Subscripts

B = bursting
m = mean value
R = reattachment
S = separation
SB = sub-bursting
T = transition
1 = upstream
2 = downstream
θ = circumferential

Presented as Paper 79-0285 at the AIAA 17th Aerospace Sciences Meeting, New Orleans, La., Jan. 15-17, 1979; submitted Jan. 30, 1979; revision received July 3, 1979. Copyright © American Institute of Aeronautics and Astronautics, Inc., 1979. All rights reserved. Reprints of this article may be ordered from AIAA Special Publications, 1290 Avenue of the Americas, New York, N.Y. 10019. Order by Article No. at top of page. Member price $2.00 each, nonmember, $3.00 each. **Remittance must accompany order.**

Index categories: Aerodynamics; Boundary-Layer Stability and Transition.

*Project Engineer. Member AIAA.

Introduction

FOR moderately thick airfoil sections ($t/c = 0.9$-0.18) at angles of attack near stall, there occurs a suction peak near the leading edge. If the surface of the airfoil is smooth and the freestream turbulence is low, the laminar boundary layer can separate due to the pressure gradient aft of the velocity peak. Transition then occurs in the separated shear layer, and the flow reattaches to the airfoil surface as a turbulent boundary layer. This flow phenomenon is termed a short laminar separation bubble. A sufficient increase in the angle of attack or decrease in Reynolds number can cause the turbulent free shear layer to fail to reattach. This is called short bubble "bursting" and is the cause of abrupt leading edge stall. An example of this is shown in Fig. 1 for a NACA 63_1-012 airfoil section. This figure shows the sudden decrease in lift over drag ratio that occurs with abrupt leading edge stall. After bursting, the free shear layer may reattach as a long bubble or remain separated, depending on the local pressure gradient and Reynolds number. However, in all instances, short bubble bursting causes a significant reduction in the suction peak, and therefore lift, an increase in drag, and fixes the maximum angle of attack possible for an airfoil section for any given condition of Reynolds number and freestream turbulence. It would be of obvious benefit to be able to predict the development and bursting conditions of these separation bubbles, especially for the new series of airfoils becoming available for general aviation application. This paper presents a technique that will allow the ap-

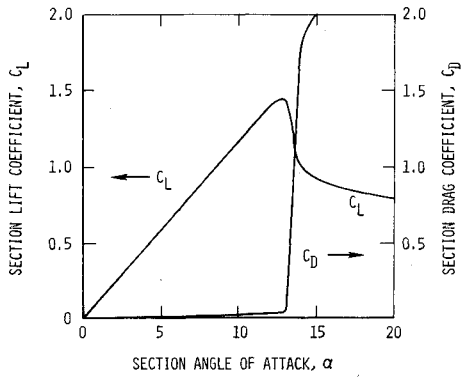

Fig. 1 Aerodynamic characteristics of a NACA 63,-012 airfoil section at a Reynolds number of 5,800,000 (Ref. 12).

proximate calculation of these important parameters, and is an adaptation of Horton's method[1] and this author's work[2] concerning Reynolds numbers effects in axial compressor blading.

Discussion of the Flow Phenomenon

This discussion was developed from a thorough review of the pertinent literature.[2] If, for the time being, we postpone consideration of the factors that define whether a bubble is short or long, the conditions necessary for the formation of a laminar separation bubble are: 1) an adverse pressure gradient of suffficient magnitude to cause laminar separation, and 2) flow conditions over the blade surface such that the boundary layer will be laminar at the separation point. Inherent in the second condition is that the airfoil surface be smooth, that the freestream turbulence level be relatively low, and that the distance between the stagnation and separation points be moderate (or more precisely, that the boundary layer Reynolds number at the laminar separation point $R_{\theta_S^*}$ be less than that required for transition). The essential features of a laminar separation bubble are illustrated in Fig. 2.

The laminar boundary layer separates from the surface at S to reattach downstream at the point R. Between the points S and R the flow may be divided into two main regions: 1) the free shear layer, contained between the outer edge S″T″R″ of the viscous region and the mean dividing streamline ST′R, and 2) the recirculation bubble contained between the mean dividing streamline and the blade surface STR. These two regions may then be further subdivided into parts upstream and downstream of the transition point T. Upstream of T, the free shear layer is laminar and is incapable of doing any significant diffusion, because weak viscous shear stresses operate in this region. As shown in Fig. 2 the surface velocity is practically constant between separation and transition. This constant pressure "plateau" is a general feature of the laminar part of the separated flow.

So far, we have been discussing laminar separation bubbles in general, without making any distinction between short and long bubbles. Perhaps the most basic way of making this distinction was proposed by Tani,[3] who has suggested that the difference between a short and long bubble lies in their effect upon the overall velocity and pressure distribution. The short separation bubble has only a slight effect upon the pressure distribution. Outside of the short bubble region the pressure distribution is a close approximation to the inviscid distribution about the profile, apart from a slight reduction in the magnitude of the suction peak ahead of separation. On the other hand, a long bubble is one which interacts with the exterior flow to such an extent that the pressure distribution is appreciably modified from the inviscid model in a way that the velocity peak and circulation are decreased. This difference can be seen in Fig. 2c, where Gaster's[4] series II pressure distributions have been plotted.

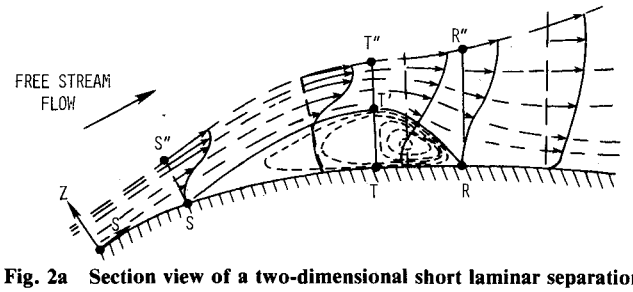

Fig. 2a Section view of a two-dimensional short laminar separation bubble, z scale greatly exaggerated.

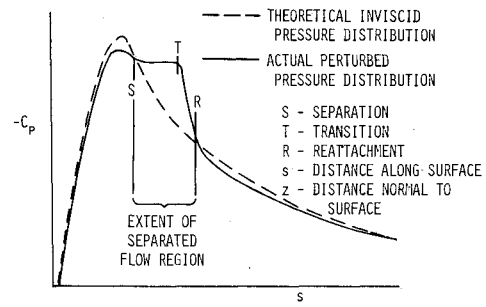

Fig. 2b The corresponding surface pressure distribution.

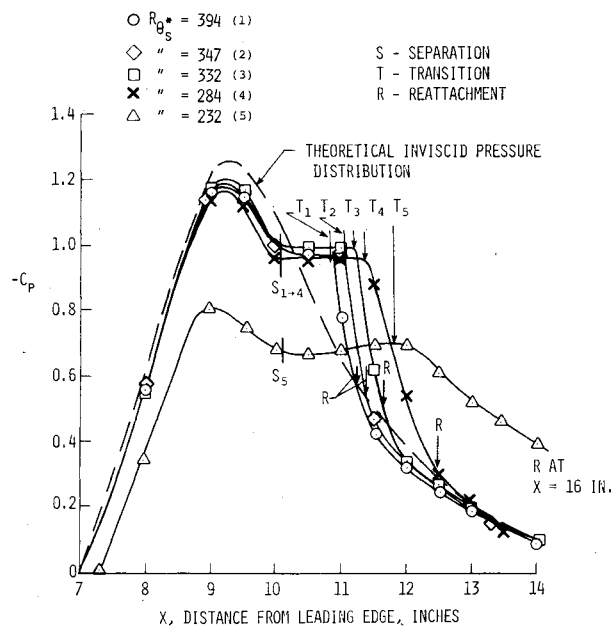

Fig. 2c Pressure distributions in the vicinity of separation bubbles for the series II experiments of Gaster,[4] bubbles 1 to 4 are short, 5 is a long bubble.

We can characterize laminar separation bubble behavior in the following way: For any given angle of attack, when the overall airfoil chord Reynolds number gets low enough, the laminar boundary layer reaches the separation point before transition is achieved. After the laminar boundary layer separates, it forms a laminar free shear layer that eventually undergoes transition to turbulence. The turbulent free shear layer is able to do enough diffusion by entrainment of high energy freestream fluid to reattach to the surface as a turbulent boundary layer. This short bubble is seen as a small perturbation on the pressure distribution; its effect on the flow outside of the bubble region is minimal.

As R_c continues to decrease, the laminar free shear layer grows in length (the mechanism of this growth will be discussed in more detail in subsequent sections). This growth

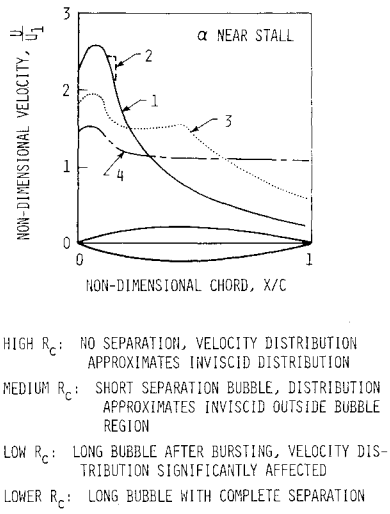

Fig. 3 Schematic of the four flow regimes possible with varying Reynolds number, 10^7-10^5, over the suction surface of an airfoil profile in low speed flow at an angle of attack near stall.

causes the turbulent free shear layer to increase diffusion to reattach at a pressure near the inviscid pressure value (see Fig. 2). Finally, R_c becomes so low and the laminar shear layer so long that the turbulent entrainment process can no longer support the diffusion required for reattachment with a value close to the invsicid pressure level. This is when the bubble starts to significantly affect the flow outside the bubble region. The velocity peak and circulation decrease, thereby reducing the pressure gradient over the bubble. This allows the turbulent shear flow to reattach as a long bubble—that is, the short bubble has burst into a long bubble.

As R_c is further lowered, the velocity peak and circulation are further decreased. Finally, the bubble is so long that reattachment on the blade surface is no longer possible. The flow is then completely separated, and there is little change to the flowfield around the profile with continued decrease of Reynolds number.

To summarize, within the angle of attack operating range of an airfoil section there are four flow regimes possible across a large Reynolds number range (disregarding trailing edge stall due to turbulent separation): 1) R_c sufficiently high for transition to occur before separation, 2) short bubble region (before bursting), 3) long bubble region (after bursting), and 4) complete separation. These four flow regimes are shown schematically in Fig. 3 for an airfoil section at constant angle of attack.

For a fixed Reynolds number, varying the angle of attack changes the pressure distribution around the airfoil and, therefore, the pressure gradient aft of the suction peak. This shifts the location of the separation bubble. If the angle of attack increases, the pressure gradient after the suction peak increases, and the short bubble moves toward the leading edge and decreases in length. This is because laminar separation occurs closer to the peak and the greater pressure gradient promotes amplification of any disturbances in the laminar boundary layer resulting in earlier transition in the free shear layer. However, in the sudden aircraft stall on departures and approach the wing angle of attack is increased to near maximum and held there while the airspeed decreases. This causes a decrease of Reynolds number and an increase in short bubble length until reattachment is not possible. At the stalling angle of attack associated with most airfoils of moderate thickness, the velocity distribution is quite "peaked" near the leading edge and the pressure gradients are very high. When the turbulent free shear layer fails to reattach, the "bursting" of the short bubble can cause a large decrease in circulation that is known as abrupt leading edge stall.

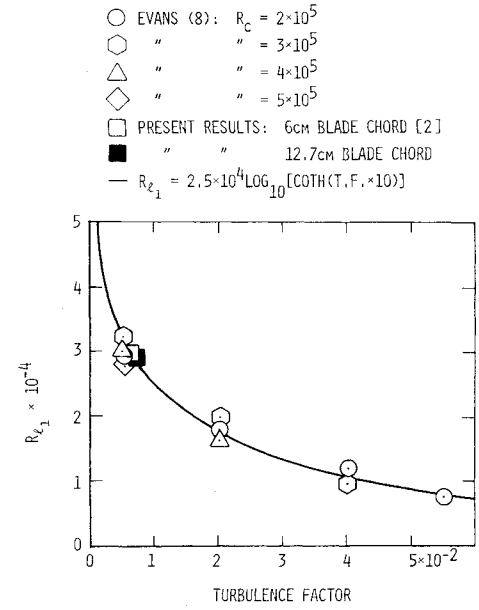

Fig. 4 Variation of Reynolds number based on transition length R_{ℓ_l} with turbulence factor TF.

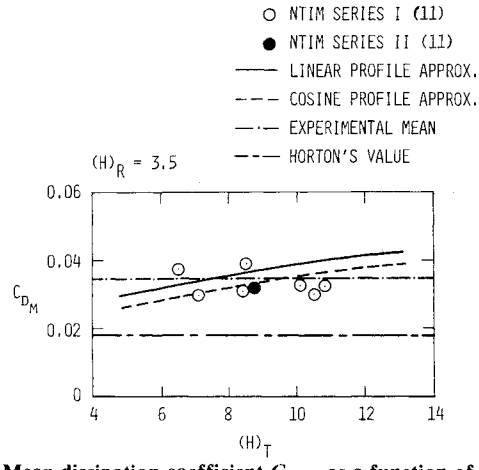

Fig. 5 Mean dissipation coefficient $C_{d(m)}$ as a function of the shape parameter at transition H_T.

Modified, Semiempirical Theory for Development and Bursting of Laminar Separation Bubbles

Equations and Discussion

The method proposed here is a modification of Horton's[1] semiempirical theory. Using Horton's theory, calculations of short bubble growth were compared with selected results of this author's research and that taken from the literature. It was found that in general Horton's method gave a delayed prediction of bursting and underestimated the losses. This was probably due to three factors: 1) inadequate transition criterion, 2) possible error in the value of the reattachment criterion, Λ_R, and 3) the low value of the mean dissipation coefficient $C_{d(m)}$. A thorough analysis was done[2] to correct these faults. The resulting modified theory is presented below.

The Laminar Part

Transition length

$$\frac{\ell_l}{\theta_s^*} = \ell_l^- = \frac{R_{\ell_l}}{R_{\theta s}^*} = \frac{2.5\times 10^4 \log_{10}[\coth(TF\times 10)]}{R_{\theta s}^*} \tag{1}$$

where

$$TF = T_{\bar{u}'}\,(C/L_s)^{1/5}$$

Growth

$$\frac{d\theta^*}{ds} \sim 0, \quad \theta_s^* \sim \theta_T^* \tag{2}$$

Turbulent Part of the Bubble

Reattachment criterion

$$(\Lambda_R) = \left(\frac{\theta^* dU_e}{U_e ds}\right)_R = \left(\frac{-C_d}{H_\epsilon(H-1)}\right)_R \tag{3}$$

$$(\Lambda)_{\text{theory}} = -0.0059$$

Length relations

$$\frac{\ell_2}{\theta_s^*} = \bar{\ell}_2 = \frac{B_1 \cdot (1-\bar{U}_{eR})}{(\bar{U}_{eR})4 - C_1}, \quad \bar{L} = \bar{\ell}_2 + \bar{\ell}_1 \tag{4}$$

$$B_1 = \frac{1}{(C_{d(m)}/4H_{\epsilon(m)}) - \Lambda_R}, \quad C_1 = (C_{d(m)}/4H_{\epsilon(m)}) \cdot B_1$$

Growth

$$\overline{\theta_R^*} = \frac{1}{(\bar{U}_{eR})^3} + \frac{C_{d(m)}}{4H_{\epsilon(m)}} \frac{\bar{\ell}_2(1-\bar{U}_{eR}{}^4)}{(\bar{U}_{eR})^3(1-\bar{U}_{eR})} \tag{5}$$

$$\bar{\ell}_2 = \ell_2/\theta_s^*, \quad C_{d(m)} \simeq 0.035, \quad H_{\epsilon(m)} \simeq 1.5 \tag{6}$$

A bar indicates normalization with respect to values at separation.

The equations in the foregoing follow from three approximations that are reasonable for a short bubble: 1) the perturbation to the inviscid velocity distribution is negligible except over the length of the bubble itself; 2) the external velocity over the laminar part of the bubble is constant to a good approximation; and 3) the external velocity falls linearly between the transition and reattachment points.

The Laminar Part

Horton concluded that there were not enough data available to take into account the effect of the freestream turbulence on the point of transition in the laminar free shear layer. He therefore chose a correlation that neglected this important parameter.

The work of Taylor,[5] Dryden et al.,[6] Schubauer,[7] and, recently, Evans[8] have indicated that the transition point for attached and free shear flow is not only a function of turbulence intensity $T_{u'}$, but also the macroscale length L_s of the flow turbulence. Therefore the turbulence factor *TF*, defined by Taylor, was used in the correlation for transition.

Using the data of Evans[8] along with that of Ref. 2, this author was able to find a correlation that relates turbulence factor (*TF*) to the Reynolds number based on transition length R_ℓ. This correlation is shown in Fig. 4. Using the correlation formula in the place of Horton's constant leads to Eq. (1).

For most wind tunnel experiments only the intensity of the turbulence is measured. For such cases the intensity can be substituted for *TF* in Eq. (1) as a first approximation since the macroscale affects the value of *TF* by only the 1/5th power. However, for unusual wind tunnel configurations or atmospheric flight experiments, significant errors could result if the macroscale is not taken into account.

Since the pressure and velocity are practically constant, and the reverse flow velocities below the laminar part are negligible, the skin friction is also very small; hence, Eq. (2).

The Turbulent Part

Using Truckenbrodt's shape parameter equation,[9] Horton derived a criterion for reattachment. He determined from the literature and his own experiments that at reattachment $H \simeq 3.5$, $H_\epsilon \simeq 1.5$, $C_d \simeq 0.222$, and $d(H_\epsilon)/dS \simeq 0$. Then Eq. (3) follows since $C_f = 0$ at reattachment. Horton then attempted to measure Λ_R experimentally. These measurements are very difficult because the velocity gradients are large and changing

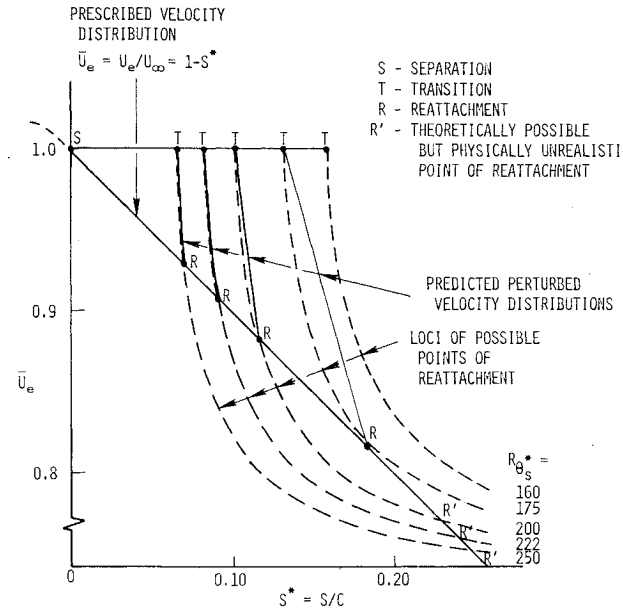

Fig. 6 Example of graphical prediction of bubble growth and bursting.

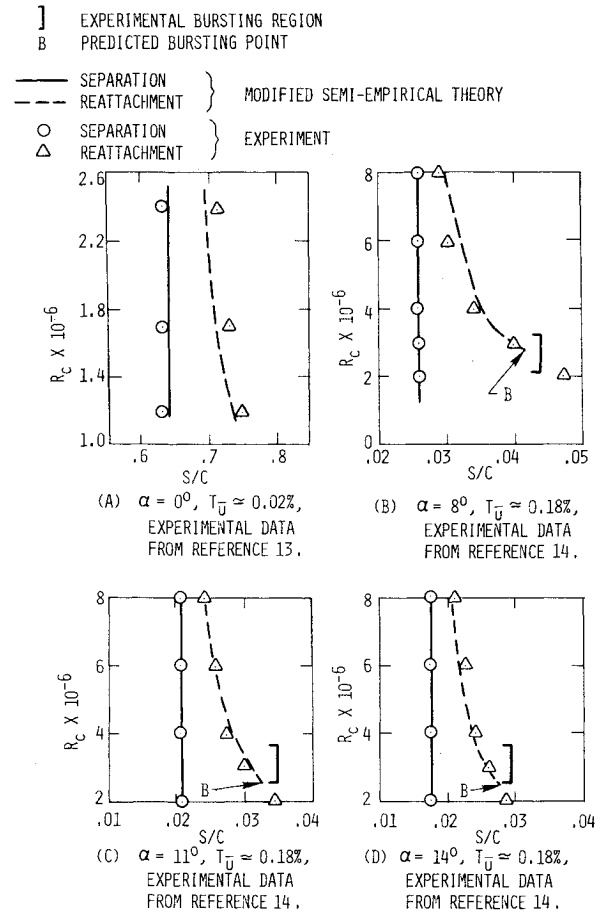

Fig. 7 Position of separation and reattachment for bubbles occurring on the suction surface of a NACA 66,3-018 airfoil at various angles of attack for low freestream turbulence intensity: modified semiempirical theory vs experiment.

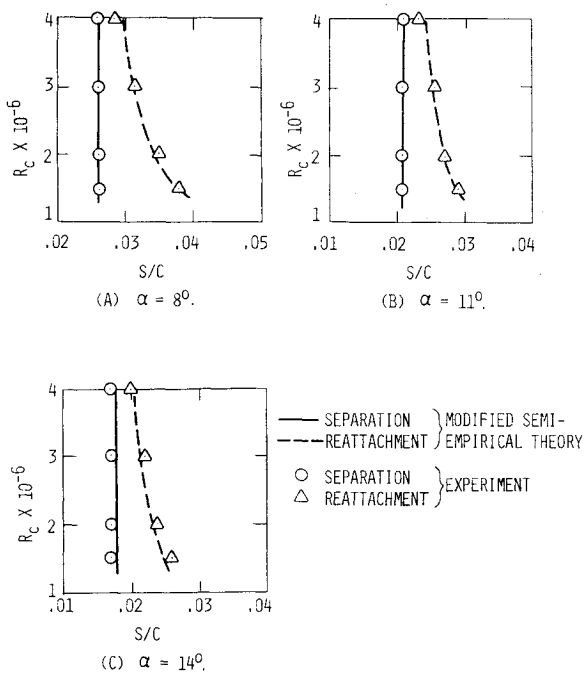

Fig. 8 Position of separation and of reattachment for bubbles occurring on the suction surface of a NACA 66,3-018 airfoil at various angles of attack for a free stream turbulence intensity of ~1.1%: modified semiempirical theory vs experiment (all experimental data taken from Ref. 11).

rapidly in the region of reattachment, and the position of reattachment is hard to determine accurately. Horton used the value determined experimentally as his reattachment criterion.

After several trials of both the theoretical and empirical values of the reattachment criterion, this author found that the theoretical value gave better agreement with experiment than the empirical. Therefore, the former was adopted for Eq. (3).

Horton found that between transition and reattachment $H_{\epsilon(m)} \simeq 1.5$. He further assumed that a mean dissipation coefficient $C_{d(m)}$, could be considered between transition and reattachment. The integral energy equation can be written as:

$$\bar{\theta}^*(\bar{U}_{e_R})^3 - 1 = \frac{C_{d(m)}}{H_{\epsilon(m)}} \int_{\bar{S}_T}^{\bar{S}_R} \bar{U}_e 3 \mathrm{d}\bar{S}$$

where the bar indicates normalization with respect to values at separation.

Linear relations for the velocity drop between transition and reattachment can be written as:

$$\bar{U}_e = 1 - (1 - \bar{U}_{e_R})\left(\frac{\bar{S} - \bar{\ell}_1}{\bar{\ell}_2}\right), \quad \left(\frac{\mathrm{d}\bar{U}_e}{\mathrm{d}\bar{S}}\right)_{T-R} = \frac{(1 - \bar{U}_{e_R})}{\bar{\ell}_2}$$

Use of the three equations in the foregoing with the definition of the Reattachment criterion, Eq. (3), leads to Eqs. (4) and (5) (see Refs. 1 or 2 for a complete derivation).

After a study of the turbulent half-jet profile of Liepman and Laufer[10] and correlating various experimental results, Horton concluded that $C_{d(m)} \simeq 0.0182$, which he subsequently used in his theory. However, the experiments of Liepman and Laufer were done for zero pressure gradient. The dissipation should be much higher in the presence of the strong adverse pressure gradient tht is present for a reattaching turbulent free shear layer.

Using linear and cosine approximations to the velocity profile in the reattaching turbulent free shear layer, this

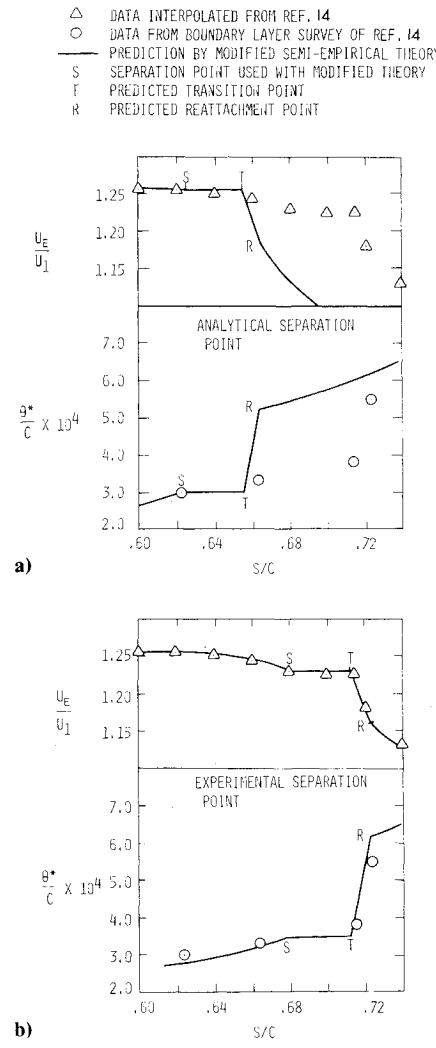

Fig. 9 Comparison of predicted and experimental velocity and momentum thickness variation through a laminar separation bubble on the surface of a NACA 66,3-018 airfoil section at $\alpha = 0$ deg, $R_c = 2 \times 10^6$, $T_u \simeq 0.18\%$ using both experimental and analytical separation points in the modified semiempirical theory.

author[2] was able to relate the dissipation coefficient with the form factor from transition to reattachment:

$$C_d \simeq 0.02\left(\frac{3H-3}{2H}\right)^3, \quad \text{linear approximation}$$

$$C_d \simeq 0.059\left(1 - \frac{1}{H}\right)^3, \quad \text{cosine approximation}$$

Then for any variation of H from transition to reattachment C_{d_m} could be evaluated by

$$C_{d(m)} = \int_T^R C_d \mathrm{d}H \Big/ \int_T^R \mathrm{d}H, \quad (H)_R \sim 3.5$$

This variation was plotted for various values of the shape parameter, along with values of $C_{d(m)}$ derived from the bubble data of Ntim.[11] This is shown in Fig. 5. As can be seen over the range of interest, the variation of $C_{d(m)}$ using the two profile approximations is small. The experimental data indicate that $C_{d(m)}$ could be taken constant throughout the reattachment process and that

$$C_{d(m)} \sim 0.035 \tag{6}$$

This is almost twice Horton's value.

The curves of ℓ_2 vs U_{eR} for various $R^*_{\theta(s)}$, given by Eq. (4), may be described as the loci of possible points of reattachment (LPPR). Figure 6 shows this for a bubble on a linear velocity distribution. The intersection of the LPPR with the inviscid velocity distribution determines the reattachment points. It is seen as Reynolds number decreases that a progressive expansion of the bubble occurs until the curve finally becomes tangential. Below this Reynolds number reattachment is not possible. This point of tangency is taken as the bursting point. The other reattachment points shown after this are not physically realistic, since this would imply that for a fixed angle of attack a short laminar bubble would get shorter as bursting is approached. This is contrary to experimental observation.

Evaluation

The modified semiempirical theory has been used to predict the approximate bursting Reynolds number and bubble lengths for airfoil sections. An example of these predictions is seen in Figs. 7 and 8. There the bubble lengths and bursting regions on a NACA 66, 3-018 airfoil section are compared for various angles of attack and turbulence intensities as a function of Reynolds number. The three bursting regions were estimated from the pressure coefficient distributions in Ref. 14. Bursting is assumed to have occurred when the peak pressure coefficient and/or the airfoil circulation dropped significantly from the high Reynolds number values. Since the Reynolds number varied at least by 10^6 between readings, an experimental bursting region is presented in Figs. 7 and 8. Nevertheless, the agreement between the prediction and experiment is reasonably good.

Figure 9 shows a comparison between predicted and experimental velocity and momentum thickness variation through a laminar separation bubble aft of the midchord on a NACA 66,3-018 airfoil section.[14] Figure 9a compares the semiempirical method to experiment using the separation point predicted from an inviscid velocity distribution[15] coupled with a laminar/turbulent boundary layer method,[16] while Fig. 9b shows the result of using the start of the constant pressure "plateau" as the separation point. It is seen that the variation is altered in the chordwise direction and highlights the importance of the location of the separation point. However, the predicted values at separation and reattachment are reasonable in both cases and would serve as a reasonable tie between attached laminar and turbulent boundary layer conditions.

Discussion and Conclusion

The modified semiempirical theory presented here has made reasonable predictions of the growth and bursting of laminar separation bubbles on the NACA 66,3-018 airfoil section at various angles of attack. As such it could be a useful tool for the prediction of abrupt stall. A comparison of predicted and experimental velocity and momentum thickness variation through a bubble region has shown the sensitivity of the calculations to the proper input conditions. The data of Figs. 7 and 8 were taken from chordwise plots of bubble lengths in Refs. 13 and 14, while those of Fig. 9 came from this author's interpolation of velocity distributions and reduction of boundary layer velocity profiles in Ref. 14. The need for interpolation came about because an experimental pressure distribution was not available for the Reynolds number at which the boundary layer measurements were taken. Therefore, there is some experimental uncertainty about the separation and reattachment locations for Fig. 9. Unfortunately, this author was unable to locate any additional data that had not already been used to make up the correlation[1,2] that give the turbulence level and development of the boundary layer through the laminar bubble region in sufficient detail to be usable for comparison with the semiempirical theory. To develop this and other techniques for calculating the flow through the bubble, experimental data must be collected in sufficient detail to further verify these methods. Furthermore, these experiments could be used to confirm that the empirical constants used are applicable to the extremes of the practical situations that will be encountered, especially for the very low turbulence flows that are found in free flight situations.

The proper use of this technique requires the availability of reliable methods of calculating pressure/velocity distributions and laminar/turbulent boundary layers. Current inviscid predictors are generally unable to calculate velocity peaks reliably near the leading edge of airfoils at high angles of attack. This can cause an error in the location of the separation point, which in turn could cause an error in the predicted bursting Reynolds number and/or angle of attack. Finally, the freestream turbulence intensity and scale and the surface roughness of the airfoil should be specified. There are very few data available that details these last factors.

A possible solution to the problem mentioned above would be to use a viscid/inviscid interaction scheme, such as the numerical techniques reported by Briley and McDonald[17] and Crimi and Reeves,[18] that takes into account the effect of the displacement thickness of the boundary layer and bubble on the external flow. The semiempirical theory presented herein does not attempt to do this, although it certainly can be used with success in an interactive manner with a potential flow code as shown by Hansen et al.[19] for airfoils in cascade. Due to its simplicity the present method does have a computational advantage compared to the numerical techniques cited. Indeed, given an inviscid velocity distribution, the laminar boundary layer up to separation and the bubble region can be computed with a hand calculator using Thwaites[20] and the present method.

Acknowledgments

The author wishes to express his gratitude for the support of the von Kármán Institute and Nielsen Engineering & Research, Inc. during the preparation of this work.

References

[1] Horton, H. P., "An Semi-Empirical Theory for the Growth and Bursting of Laminar Separation Bubbles," Aeronautical Research Council, Britain, Current Paper 1073, 1969.

[2] Roberts, W. B., "A Study of the Effect of Reynolds Number and Laminar Separation Bubbles on the Flow through Axial Compressor Cascades," D.Sc. Thesis, U. Libre de Bruxelles and VKI, May 1973; summarized in the *ASME Journal of Engineering for Power*, April 1975, pp. 261-274.

[3] Tani, I., "Low Speed Flows Involving Bubble Separations," *Progress in Aeronautical Science*, Pergamon Press, 1964, pp. 70-103.

[4] Gaster, M., "The Structure and Behavior of Laminar Separation Bubbles," NPL Aero Report 1181, ARC 28.226, 1966.

[5] Taylor, G. I., *Proceedings of the Royal Aeronautical Society*, Vol. 56, 307, 1936. Also *Proceedings of the 5th International Congress of Applied Mechanics*, 1938, p. 294.

[6] Dryden, H. L., Schubauer, G. B., Mock, W. C., and Skramstad, H. K., "Measurement of Intensity and Scale of Wind-Tunnel Turbulence and Their Relation to the Critical Reynolds Numbers of Spheres," NACA Rept. 581, 1937.

[7] Schubauer, G. B., "Air Flow in the Boundary Layer of an Elliptic Cylinder," NACA Rept. 652, 1937.

[8] Evans, B. J., "Effects of the Free-Stream Turbulence on Blade Performance in a Compressor Cascade," Cambridge University, Engineering Department Turbo/TR25, 1971.

[9] Truckenbrodt, E., "An Approximate Method for the Calculation of the Laminar and Turbulent Boundary Layer by Simple Quadrature for Two-Dimensional and Axially Symmetric Flow," *Journal of Aeronautical Science*, Vol. 19, June 1952.

[10] Liepman, H. W. and Laufer, J., "Investigation of Free Turbulent Mixing," NACA TN 1257, 1947.

[11] Ntim, B. A., "A Theoretical and Experimental Investigation of Separation Bubbles," Ph.D. Thesis, University of London, Queen Mary College, 1969.

[12]McCullough, G. B. and Gault, D. E., "Examples of Three Representative Types of Airfoil-Section Stall at Low Speed," NACA TN 2502, 1951.

[13]Bursnall, W. J. and Loftin, L. K., "Experimental Investigation of Localized Regions of Laminar Boundary Layer Separation," NACA TN 2338, 1951.

[14]Gault, D. E., "An Experimental Investigation of Regions of Separated Laminar Flows," NACA TN 3505, 1955.

[15]Van den Braembussche, R., "Martensen's Method for Calculation of Incompressible Potential Flow in Cascade," von Kármán Institute, CN 80, 1970.

[16]Papailiou, K. P., "An Investigation on Le Foll's Method Used for Blade Optimization Based on Boundary Layer Concepts," von Kármán Institute, TN 61, 1969.

[17]Briley, W. R. and McDonald, H., "Numerical Prediction of Incompressible Separation Bubbles," *Journal of Fluid Mechanics*, Vol. 69, June 1975, pp. 631-656.

[18]Crimi, P. and Reeves, B. L., "Analysis of Leading-Edge Separation Bubbles on Airfoils," *AIAA Journal*, Vol. 14, Nov. 1976, pp. 1548-1555.

[19]Hansen, E. C., Serovy, G. K., and Sockol, P. M., "Axial-Flow Compressor Turning Angle and Loss by Inviscid-Viscous Interaction Blade-to-Blade Computation," ASME Paper No. 79-GT-5, March 1979.

[20]Thwaites, B., "Approximate Calculation of the Laminar Boundary Layer," *Aeronautical Quarterly*, 1, 1945.

From the AIAA Progress in Astronautics and Aeronautics Series..

EXPERIMENTAL DIAGNOSTICS IN COMBUSTION OF SOLIDS—v. 63

Edited by Thomas L. Boggs, Naval Weapons Center, and Ben T. Zinn, Georgia Institute of Technology

The present volume was prepared as a sequel to Volume 53, *Experimental Diagnostics in Gas Phase Combustion Systems*, published in 1977. Its objective is similar to that of the gas phase combustion volume, namely, to assemble in one place a set of advanced expository treatments of the newest diagnostic methods that have emerged in recent years in experemental combustion research in heterogenous systems and to analyze both the potentials and the shortcomings in ways that would suggest directions for future development. The emphasis in the first volume was on homogenous gas phase systems, usually the subject of idealized laboratory researches; the emphasis in the present volume is on heterogenous two- or more-phase systems typical of those encountered in practical combustors.

As remarked in the 1977 volume, the particular diagnostic methods selected for presentation were largely undeveloped a decade ago. However, these more powerful methods now make possible a deeper and much more detailed understanding of the complex processes in combustion than we had thought feasible at that time.

Like the previous one, this volume was planned as a means to disseminate the techniques hitherto known only to specialists to the much broader community of reesearch scientists and development engineers in the combustion field. We believe that the articles and the selected references to the current literature contained in the articles will prove useful and stimulating.

339 pp., 6 × 9 illus., including one four-color plate, $20.00 Mem., $35.00 List

TO ORDER WRITE: Publications Dept., AIAA, 1290 Avenue of the Americas, New York, N.Y. 10019